High-Sensitivity Piezoresistive Pressure Detection by a Depletion Channel Metal-Oxide-Semiconductor Transistor [MOST] Bridge

T. Mohácsy*, M. Ádám, S. Kulinyi[1] and I. Bársony

Research Institute for Technical Physics and
Materials Science MTA-MFA, P.O. Box 49, H-1525 Budapest, Hungary
[1]WESZTA-T Ltd., Lívia u. 8. H-1025 Budapest, Hungary

Membrane thickness and resistivity limitation in the sensitivity of piezoresistive pressure sensors can be overcome by the proposed depletion-mode p-channel metal-oxide-semiconductor transistor (MOST) bridge elements. After an overview of the theoretical background, the principle of operation and the device characteristics are discussed. Using the novel design with the same membrane thickness, over an order of magnitude increase in sensitivity was achieved. Cyclic stressing (30 times) at 25°C and 80°C by 500 pressure pulses (0–1.6 bar), respectively resulted in excellent stability of the device.

1. Introduction

Conventional piezoresistive bridges contain diffused resistors on the order of 2–10 kΩ with a typical current bias of 1–3 mA. This corresponds to the requirement of an optimum piezoresistive coefficient (π_{44})[1,2] achieved at doping levels of 3×10^{18} cm^{-3}. The obtainable sensitivity for a membrane thickness of 300 μm is about 1.2 mV/bar. In low-pressure applications these values impose a severe limitation, since any further improvement is only possible at the cost of the final processing yield using thinner membranes. This was the motivation for the proposal of a depletion-mode [MOST] bridge-type pressure sensor.[3] This work describes the operational principle, design, realisation and evaluation of a novel high-sensitivity pressure sensor.

---

*Corresponding author's e-mail address: mohacsy@mfa.kfki.hu

2.   Theoretical

2.1 *Principle of operation*

By replacing the diffused resistors in the bridge shown in Fig. 1 by p-channel depletion transistor two-poles (gate and source shortened), optimum π_{44} conditions can be maintained in the resistive channel. To obtain maximum sensitivity, similar to the conventional Wheatstone bridge arrangement, the channels of the MOSTs follow the <110> direction on the (100)-oriented silicon substrate, and they are placed along the circle of maximum pressure sensitivity.[4] In the case of resistors, the relatively large dimensions inhibit optimum placing, while in the novel scheme, the optimum is easier to realise due to the comparatively smaller channel area of the MOSTs.

The depletion device has the same carrier mobility as the diffused resistors, i.e., in the linear region, the resistance of the channel largely corresponds to that of the diffused resistors in the conventional device.[5] The channel shortening effect, however, determines a differential resistance that is several orders of magnitude higher. The pressure sensitivity of the bridge might, therefore, be increased proportional to the enhancement of resistance.

2.2 *Small signal performance*

In Fig. 2, the setting of the operation point can be followed for the half-bridge of depletion MOSTs. Without external pressure, the operation point is (V_0, I_0) with $V_0=V_D/2$. Applying a pressure P shifts the operation point by ΔV.
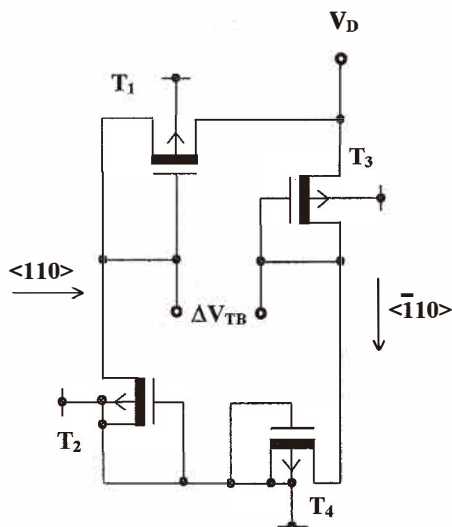
Fig. 1.   Depletion transistor-bridge with the MOST channels aligned in the <110> direction on the (100)-oriented silicon substrate.
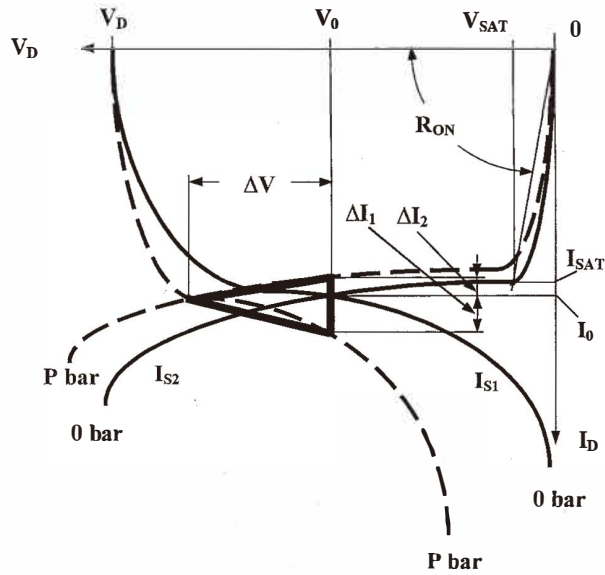
Fig. 2.   Modification of the characteristics of the depletion transistor half-bridge due to pressurizing the silicon membrane. Note that the "load device" biased to V_0 is prone to the body effect.

$$\Delta V = \frac{\Delta I_0}{g_D + g_L} = \Delta I_0 \cdot r, \tag{1}$$

where

$$\Delta I_0 = \Delta I_1 + \Delta I_2 \tag{2}$$

$$g_D = \frac{1}{r_D} \cong \frac{\Delta I_{S2}}{\Delta V_D}$$

$$g_L = \frac{1}{r_L} \cong \frac{\Delta I_{S1}}{\Delta V_D}$$

$$r = r_D \times r_L$$

$$r_L = r_{L0} \times r_{mB}$$

$$g_{mB} = \frac{1}{r_{mB}} = \frac{\Delta I_{S1}}{\Delta V_{SB}},$$

with ΔI_0 being the sum of the current shift in the saturation characteristics and g_D, g_L and g_{mB} denoting the differential conductance for the "driver" and "load" devices as well as the transconductance of the substrate-channel junction. The corresponding differential resis-

tances are r_D, r_L and r_{mB}. Due to the effect of the body bias on the characteristics of the "load" device, the differential resistance r_L is composed of two terms: one related to the nonbiased case (r_{L0}) and the other accounting for the source bias (r_{mB}). The term r stands for the differential resistance of the parallel branches.

The thickly drawn general triangle approximates the nonlinear saturation characteristics in the "driver" and "load" devices by straight line-sections in Fig. 2. The sections are in fact secants of the nonlinear saturation characteristics; their slope corresponds to the integral average of the differential conduction in the respective devices. In the same manner, the conductance ($1/R_{ON}$) in the linear region can also be deduced. This implies the possibility of constructing a small signal equivalent circuit (which is shown in Fig. 3) with g_m as the forward conductance of the "driver" transistor. ΔR_{ON} denotes the change of the resistance in the linear region of the "driver" transistor as a consequence of the pressure on the membrane.

The output voltage is given by eq. (1), while the control voltage is:

$$\Delta V_{ON} = I_{SAT} \cdot \Delta R_{ON}$$

If ($r_{mB} \to \infty$) and ($r_D = r_{L0}$), then $\Delta V \to 1/2 \cdot \Delta I_0 \cdot r_{L0}$.

This indicates that without the body effect, the triangle in Fig. 2 becomes an isosceles triangle and the amplification increases. In the saturation region with the gradual channel approximation we can write:

$$I_S = I_{SAT} \cdot \varphi(V_D), \qquad (3)$$

and

$$I_{SAT} = \frac{\beta}{2} \cdot V_T^2,$$

as the gate is connected to the source thus $V_G = 0$,
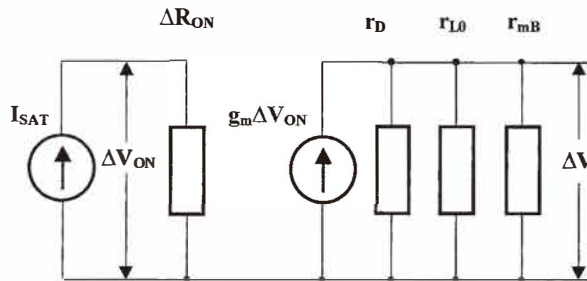
Fig. 3.   Small signal equivalent circuit of the pressurized half-bridge with the differential parameters derived from Fig. 2. The second current generator on the right is controlled by pressure via the on-resistance change ΔR_{ON}.

$$\beta = \frac{w}{L} \cdot C \cdot \mu, \quad C = C_{OX} \times C_D$$

$$\varphi(V_D) = \left(1 - \lambda \cdot \sqrt{V_D - V_{SAT}}\right)^{-1}$$

$$\lambda = \frac{1}{L} \sqrt{\frac{2\varepsilon_{Si}}{qN}},$$

where β is the well-known transistor constant with the channel geometry terms (w, L) and the mobility μ. The term V_T is the threshold voltage, C_{OX} and C_D the specific oxide capacitance and average capacitance of the surface depletion region in the operating point, respectively, ε_{Si} the dielectric constant of silicon and N the average doping concentration in the conductive channel.

2.3 *Equivalent circuit*

If the transistors are arranged parallel and perpendicular to the <110> direction and the radial stress component (σ_R) is much higher than the tangential one (σ_T) on a circle with radius $R_N \le r_M < a/2$ (see Fig. 4), then the resulting stress σ is reduced to the radial contribution: $\sigma \cong \sigma_R(P, r)$. In Fig. 4, the conditions at $P = 10$ bar were considered, but the value of R_N is independent of the pressure.[4] We assume that in the p-channel devices the pressure P, and thereby the stress σ, has negligible influence on the hole concentration.[5] The transistors are constructed such that the drain and the gate-body voltages also have no effect on the carrier mobility μ. Consequently,
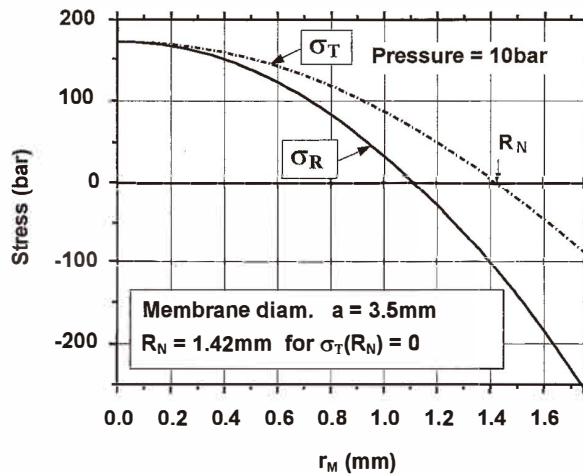
Fig. 4.   Radial (σ_R) and tangential (σ_T) stress developed in the membrane with a load of 10 bar. The term R_N is the radius of the circle, outside of which the bridge elements are placed.

$$\frac{\vartheta p_0}{\vartheta \sigma} \cong 0, \quad \frac{\vartheta \mu}{\vartheta V_\mathrm{D}} \cong 0 \text{ and } \frac{\vartheta \mu}{\vartheta_\mathrm{GB}} \cong 0, \tag{4}$$

where p_0 is the hole concentration in the channel. The shift in the saturation current ΔI_0 is calculated from constructing the differential of eq. (3) at point $V_\mathrm{D} = V_0$, taking into account eq. (2):

$$\Delta I_0 = 2 \cdot I_0 \left(\frac{\Delta K}{K_0} + \frac{\Delta \mu}{\mu_0} \right),$$

in this case:

$$\frac{\Delta K}{K_0} \frac{1}{\sigma} = -\frac{1}{2} S_{44}, \quad K = \frac{w}{L} \text{ and}$$

$$\frac{\Delta \mu}{\mu_0} \frac{1}{\sigma} \cong \pm \frac{1}{2} \pi_{44}, \tag{5}$$

where S_{44} is the compliance constant, and π_{44} is the average piezoresistance coefficient.[2] Its sign depends on the direction of the strain with respect to the orientation of the channel of the transistors (+ means longitudinal, − means transversal),

$$\Delta I_0 = -I_0 \cdot \sigma \cdot (\pi_{44} + S_{44}) \cong -I_0 \cdot \pi_{44} \cdot \sigma \text{ as } S_{44} \cong 0$$

in silicon. The output voltage of the MOST bridge is twice the value of eq. (1); therefore,

$$\Delta V_\mathrm{TB} \cong -2 \cdot I_0 \cdot \pi_{44} \cdot \sigma \cdot r = -2 \cdot I_\mathrm{SAT} \cdot \varphi(V_0) \cdot \pi_{44} \cdot \sigma \cdot r. \tag{6}$$

The voltage difference ΔV_RB is obtained with a conventional resistor-type bridge with the branch elements R_ON according to Fig. 2. In the case of this linear resistive bridge, the output voltage is calculated as

$$\Delta V_\mathrm{RB} = 2 \cdot I_\mathrm{SAT} \cdot \Delta R_\mathrm{ON},$$

with

$$\Delta R_\mathrm{ON} \cong \frac{1}{2} \cdot R_\mathrm{ON} \cdot \pi_{44} \cdot \sigma, \text{ (as in ref. (4))}$$

thus

$$\Delta V_\mathrm{RB} = I_\mathrm{SAT} \cdot R_\mathrm{ON} \cdot \pi_{44} \cdot \sigma \tag{7}$$

where

$$R_\mathrm{ON} = \frac{V_\mathrm{SAT}}{I_\mathrm{SAT}} = \frac{1}{\beta \cdot V_\mathrm{T}}.$$

The resulting gain in the depletion MOST bridge A_TB from eqs. (6) and (7) is:

$$A_{\text{TB}} = \frac{\Delta V_{\text{TB}}}{\Delta V_{\text{RB}}} \cong -2\frac{r}{R_{\text{ON}}} \cdot \varphi(V_0). \tag{8}$$

The higher the ratio of the bridge differential resistance to the linear on-resistance, the higher the obtained gain. The forward conductance g_{m} from eq. (8) with $A_{\text{TB}} = g_{\text{m}} \cdot r$ is

$$g_{\text{m}} = \frac{\Delta I_0}{\Delta V_{\text{ON}}} \cong -2\frac{\varphi(V_{\bullet})}{R_{\text{ON}}} \cong -2 \cdot \varphi(V_0) \cdot \beta \cdot V_{\text{T}}. \tag{9}$$

These calculations allow the construction of an equivalent circuit according to Fig. 5, in which the forward conductance of the additional transistors T_X has to be $g_{\text{mX}} = g_{\text{m}}/2$.

$$g_{\text{mX}} = \frac{\vartheta I_{\text{S}}}{\vartheta V_{\text{GX}}} = \beta_{\text{X}} \cdot (V_{\text{GX}} - V_{\text{T}}) \cdot \varphi(V_0) = \frac{1}{2} \cdot g_{\text{m}} = -\varphi(V_0) \cdot \beta \cdot V_{\text{T}} \tag{10}$$

Hence the gain of the circuit is

$$A_{\text{EQ}} = 2 \cdot g_{\text{mX}} \cdot r = -2 \cdot \varphi(V_0) \cdot \beta \cdot V_{\text{T}} \cdot r. \tag{11}$$

The equivalent circuit of the proposed depletion transistor bridge is shown in Fig. 5. It consists of a linear R_{ON} resistor bridge with an output signal of ΔV_{RB} and a differential amplifier composed of the same depletion transistors as those designed for the MOST bridge ($T_1....T_4$), with two additional transistors T_X as input devices. The forward conductance of T_X is calculated according to eq. (10) and the gain of the differential stage A_{EQ} by eq. (11), which corresponds to the gain A_{TB} of the MOST bridge described by eq. (8).

2.4   *Thermal drift*

The novel nonlinear pressure-sensing device composed of a linear piezoresistive sensor and an amplifier is prone to thermal drift. Consequently, the output voltage of the MOST bridge is more dependent on the temperature than that of the conventional piezoresistive bridge, which originates from the temperature dependence of the piezoresistive coefficient. The thermal behaviour of the output voltage ΔV is composed from the temperature dependence of the intrinsic carrier concentration $n_i(T)$, the band-gap energy $E_g(T)$, as well as from the pressure-sensitive mobility $\mu(T, P)$.

$$\Delta V(T, P) = \text{const}_1 \cdot \mu(T, P) \cdot f\left[n_i(T), E_g(T)\right]$$

$$\mu(T, P) = \mu_0(300, P) \cdot \left(\frac{300}{T}\right)^{\frac{3}{2}}$$

$$\Delta V_{\text{REF}}(T) = \text{const}_2 \cdot \mu(T) \cdot f\left[n_i(T), E_g(T)\right]$$
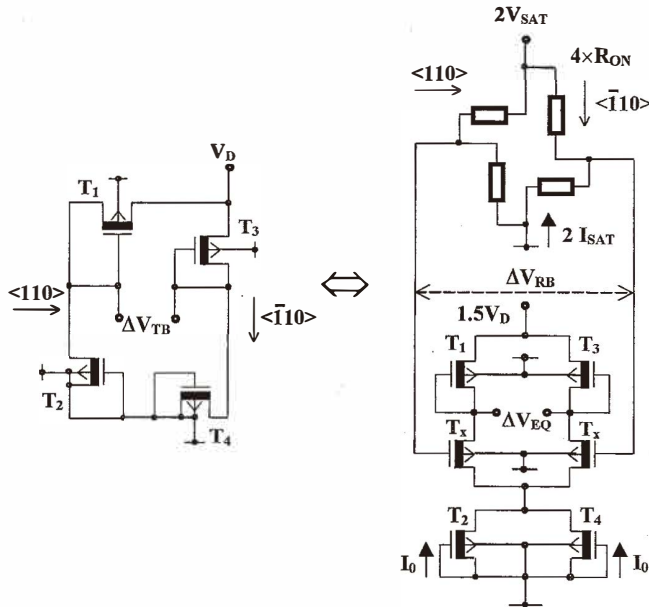
Fig. 5.   Equivalent circuit constructed for the novel depletion MOST bridge using the resistive bridge (R_{ON}) output amplified by a differential amplifier built up from $T_1...T_4$ and two additional driver depletion MOSTs, T_X.   The forward conductance of T_X as well as the gain of the system is given by eqs. (10) and (11).

$$\mu(T) = \mu_0(300) \cdot \left(\frac{300}{T}\right)^{\frac{3}{2}}$$

$$\frac{\Delta V(T,P)}{\Delta V_{REF}(T)} = \text{const} \cdot \frac{\mu_0(300,P)}{\mu_0(300)} \tag{12}$$

The effect of temperature on the pressure characteristics is simulated in the temperature range of $T = -123...+127°C$ for the case of the MOST bridge without the body effect, and for the practical case with the body effect in Fig. 6.   Equation (12) describes a way to eliminate this adverse temperature dependence by comparing the temperature and pressure dependent output $\Delta V_{TB}(T, P)$ with a "pressure-independent" reference voltage $\Delta V_{REF}(T)$. This reference can be obtained from a MOST bridge of the same dimensions realised on the same chip (equal T), but placed outside the pressurised membrane ($P = $ const.).   The corresponding electronic circuitry is shown in Fig. 7.   The temperature-independent output signal $C \cdot \Delta V(P)$ is calculated by eq. (12).   The operational amplifiers with the open-loop gain A provide the amplified output signals, and the reciprocal value of the reference signal is generated by the combination of the third operational amplifier with the input transistor
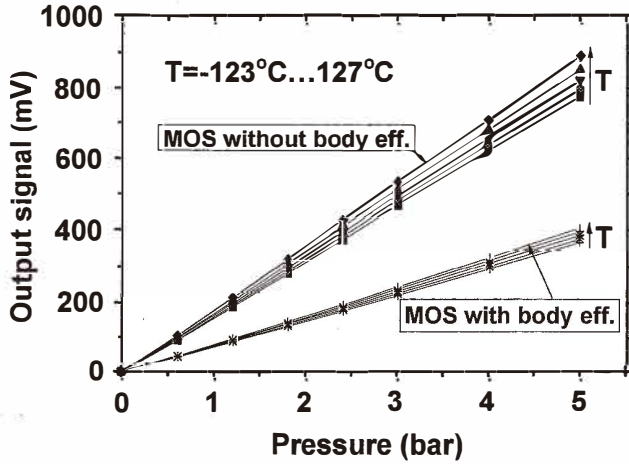
Fig. 6.   Simulated effect of temperature on pressure characteristics for the practical case (with the body effect) and the optimum case (without the body effect).
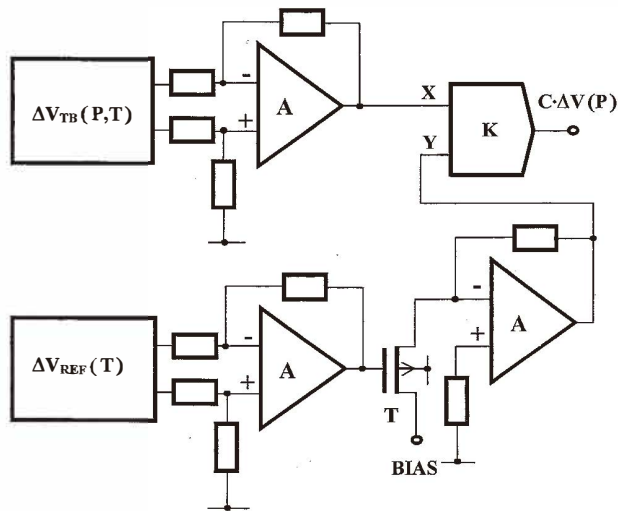
Fig. 7.   Scheme of temperature compensation for the nonlinear MOST bridge. The reciprocal value of the reference voltage $\Delta V_{REF}(T)$ is taken from the enhancement MOS transistor, while the multiplication of the amplified signals is carried out by the multiplier K.

T operated in linear mode. The multiplication of the temperature-dependent input X by the reciprocal value of the pressure-independent reference input Y is carried out in the analog multiplier K.

3.   Materials and Methods

3.1   *Design*

The described "ideal" behaviour expected with identical MOSTs is affected by the body effect of one of the MOSTs in the bridge branches in Fig. 1 (T_1 or T_3). This results in a loss of linearity, as visible on the descending saturation curve of T_1 in Fig. 8 (T_1^* denotes the characteristics of T_1 without the body effect). At the same time, the differential resistance of the channel decreases and thus, the sensitivity reduces too. Partial compensation can be achieved by the appropriate choice of pinch-off voltages (threshold voltage) V_T for the back-gated (T_1 and T_3) and nonbiased transistors (T_2, T_4). Design parameter asymmetries between T_1 and T_2 are visualised by T_1^* and T_2^* (both without the body effect). The inset in Fig. 8 shows the shift of the operating point (to the left) due to pressurising the membrane.

In Fig. 9 with linear resistor elements and in Fig. 10 with the depletion MOSTs in two-pole configuration, the bridge sensitivity ΔV vs pressure P and bridge bias V_D were
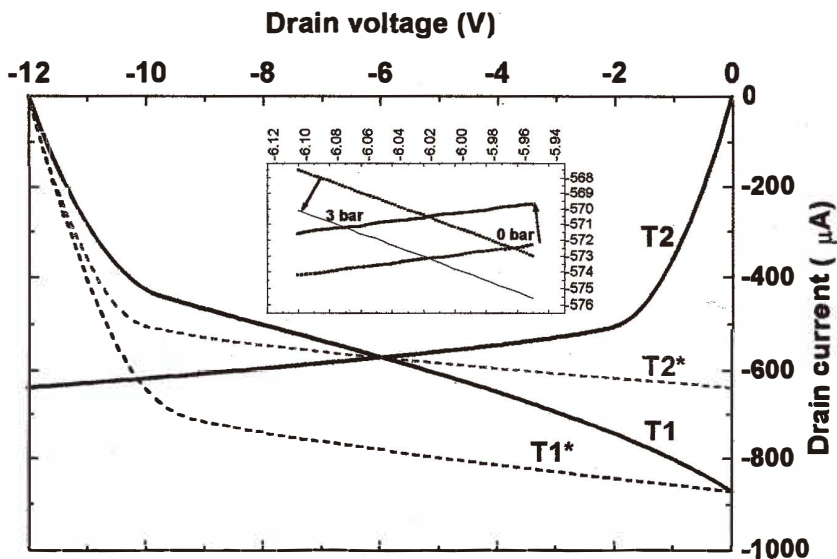
Fig. 8.   Simulated performance of the depletion transistor two-pole pressure sensor. T_1^* denotes T_1 without the body effect. Design parameter asymmetries between T_1 and T_2 are visualised by T_1^* and T_2^* (both without the body effect). The inset shows the shift of the operational point (to the left) caused by pressurising the membrane.
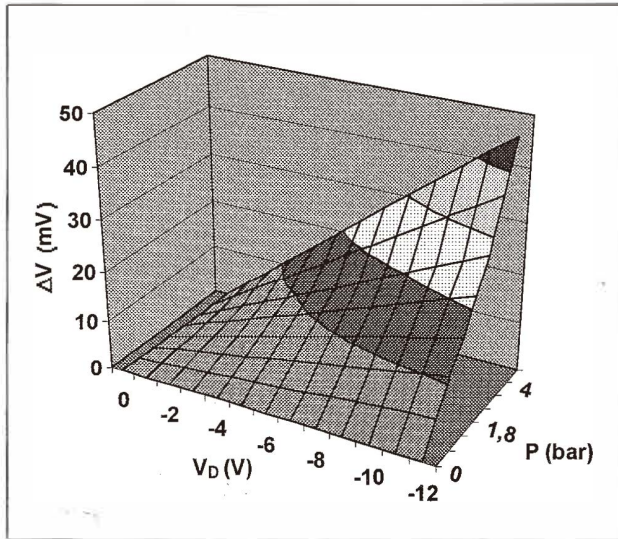
Fig. 9.   Conventional linear resistor (R=10 kΩ) Wheatstone bridge sensor performance simulated with membrane parameters: diameter = 3.5 mm, thickness = 300 μm.
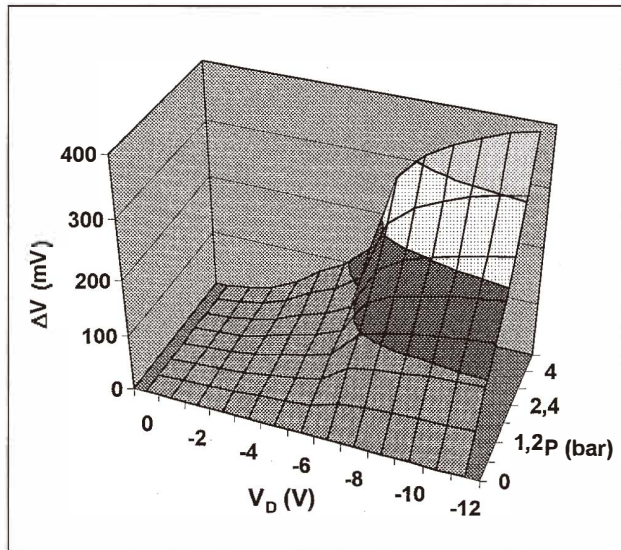
Fig.10.   MOST Wheatstone bridge pressure sensor performance calculated for membrane parameters: diameter = 3.5 mm, thickness = 300 μm, $V_{T2,4}$ = 3 V, $V_{T1,3}$ = 3.8 V, L = 20 μm, $W_{2,4}$ =172 μm, and $W_{1,3}$ = 136 μm.

simulated with SPICE. The calculation was based upon the assumption of the validity of the conditions described in eq. (4). While in Fig. 9 the linearity with pressure and supply voltage is maintained, in Fig. 10 the operation is more complex. At low supply voltages $V_D < 5$ V, the performance of this nonlinear device is similar to that of the conventional resistor bridge. After reaching saturation in the depletion MOST ($V_D > 8$ V) ΔV increases abruptly.

The linearity in the piezoresistive detection is based upon the assumption that the carrier concentration is independent of P and the linear change of mobility with pressure P follows eqs. (4) and (5). The change of saturation characteristics of the MOST for small shifts in the operational point is almost linear. The saturation region in Fig. 10 can therefore provide a multiple of the output voltage change for a given P. As an additional benefit, a sensitivity which is less dependent on V_D is noted. In the case of Fig. 9, the increased ΔV is realised with a current enhancement, and consequently, with an increased supply voltage V_D. In the novel scheme according to Fig. 1, however, the bridge current is limited by the saturation characteristics of the MOSTs and thus is nearly independent of the supply voltage V_D.

The temperature stability of the transducer characteristics is also influenced by the body effect. In the case of the resistance bridge, both branches are similarly affected by temperature; the result is therefore a virtual temperature independence of the reading. In the novel device, however, this is not the case. The pinch-off (threshold) voltage and mobility in the MOSTs are both temperatures dependent. With increased temperature, the mobility decreases, following the discussion of eq. (12), and the V_T increases in both types of MOSTs. Although these effects partially compensate each other, the temperature effect is not negligible.

3.2 Manufacturing the device

Figure 11 illustrates the cross section of the depletion MOST as a pressure-sensing element placed in the bridge configuration on the membrane at the optimum locations, i.e., on the circuit with radius R_N as shown in Fig. 4.

The device was manufactured on a (100) n-type Si wafer of 6–8 Ωcm using a conventional p-channel depletion MOST process with a 100-nm-thick gate oxide. The set threshold voltages for the bridge elements according to Fig. 1 were $V_T = 3$ V (for T_2 and T_4) and $V_T = 3.8$ V (for T_1 and T_3). The higher value was intended to compensate for the body effect. The dimensions of the MOSTs were $L = 20$ μm, $w_{2,4} = 172$ μm and $w_{1,3} = 136$ μm. The selected thickness of the membrane with a diameter $a = 3.5$ mm was $h = 300$ μm.

4.   Results and Discussion

4.1 Measured device performance

The simulated performance in Fig. 8 was verified in Fig. 12 by the measurement of the MOST half-bridge. With a load of 3 bar at $V_D = -15$ V we experimentally obtained 38 mV/bar in good agreement with the calculated 36 mV/bar at $V_D = -12$ V.

The measured results on pressurised MOST bridges are drawn in Fig. 13 at different temperatures with positive (up) and negative (down) pressure increments. Even without
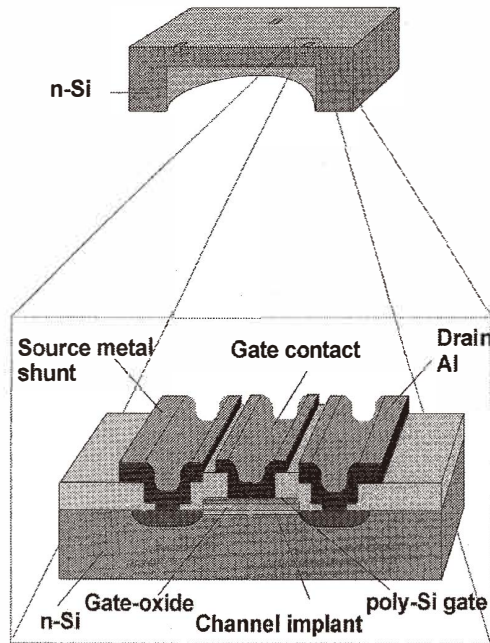
Fig. 11.   Expanded view of the MOST pressure sensor.
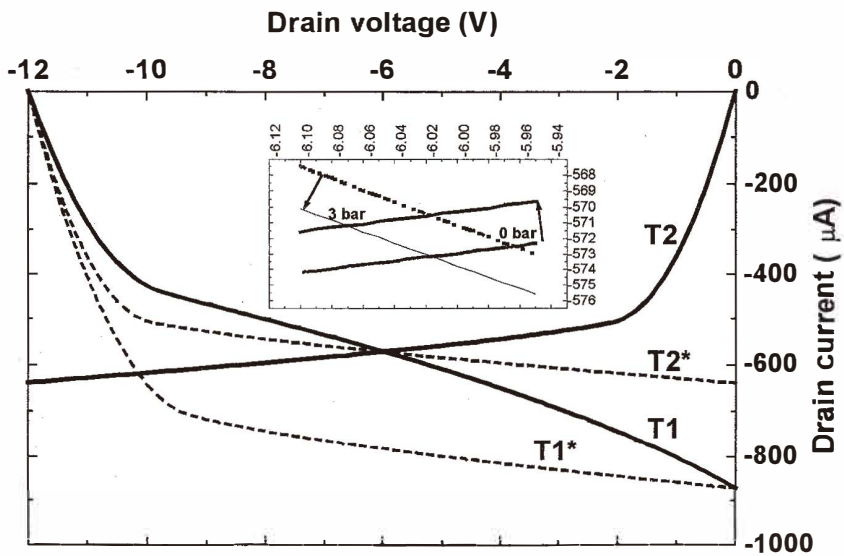
Fig. 12.   Measured performance of the realised MOST bridge in the enlarged inset. The obtained sensitivity corresponds to the calculations.
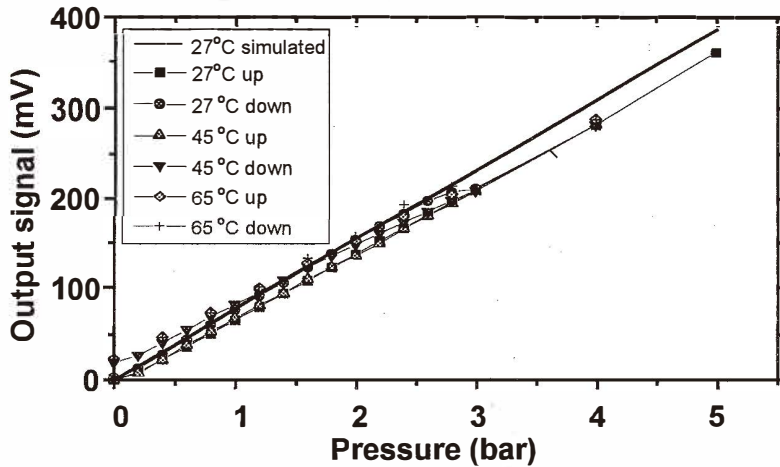
Fig. 13. Measurement results on pressurized MOST bridges with positive (up) and negative (down) pressure increments at different temperatures. Good correspondence with simulations, acceptable linearity and hysteresis were obtained. For reference, we calculated the performance of a conventional sensor on the same membrane.

specific measures, acceptable linearity was obtained, as was a good correspondence with the simulation results. Below 3 bar, however, at higher temperatures a slight hysteresis was observed due to thermal drift. Nevertheless, this drift does not exceed 15 mV over the temperature range tested.

A number of industrially mounted devices were tested by thermal and dynamic pressure stressing. The sensors were exposed to 500 pressure pulses of 0–1.6 bar at room temperature, and then to 500 pulses at 85°C. This cycle was repeated 30 times consecutively, resulting in the application of 30,000 pressure pulses. The typical characteristics recorded before and after stressing show negligible effects of the stressing on the behaviour of the device.

4.2 *Advanced structures*

Both linearity and sensitivity of the novel device are limited by the adverse body effect. The loss in linearity (very moderate) in the case of the body effect is demonstrated in Fig. 8 by comparing the operation with the "ideal" load device T_2^* vs the practical case with T_1. The loss of sensitivity is clearly visible in the simulated results in Fig. 6 in the slope differences. Therefore, attempts should be made to avoid the body effect by design.

5.   Conclusions

Extremely high sensitivity in excess of 50 mV/bar with 300-μm-thick membranes was achieved using bridge resistors formed reproducibly by depletion-mode p-channel MOSTs in two-pole configuration. Even without compensation, a tolerable temperature stability and over a one and a half order of magnitude increase in sensitivity were recorded with the same membrane thickness.

Moreover, this novel principle offers the convenience of a voltage biasing operation. This also enables the benefit of insensitivity to fluctuations in supply voltage. Cyclic dynamic stressing resulted in excellent stability of the device.

References

1   O. N. Tufte and E. L. Stelzer: J. Appl. Phys. **34** (1963) 313.
2   Y. Kanda: Sensors and Actuators A **28** (1991) 83.
3   T. Mohácsy, M. Ádám, S. Kulinyi and I. Bársony: Proc. EUROSENSORS XII 1998 (Southampton, England, 1998) p. 431.
4   O. N. Tufte, P. W. Chapman and D. Long: J. Appl. Phys. **33** (1962) 3322.
5   H. Mikoshiba: Solid State Electronics **24** (1981) 221.